The Journal of Pathology: Clinical Research
J Pathol Clin Res July 2021; **7:** 326–337
Published online 9 April 2021 in Wiley Online Library (wileyonlinelibrary.com). DOI: 10.1002/cjp2.212

ORIGINAL ARTICLE

Characterisation of cardiac pathology in 23 autopsies of lethal COVID-19

Jasmin D Haslbauer[1], Alexandar Tzankov[1], Kirsten D Mertz[2], Nathalie Schwab[2], Ronny Nienhold[2], Raphael Twerenbold[3], Gregor Leibundgut[4], Anna K Stalder[1], Matthias Matter[1] and Katharina Glatz[1]*

[1]*Pathology, Institute of Medical Genetics and Pathology, University Hospital Basel, University of Basel, Basel, Switzerland*
[2]*Institute of Pathology, Cantonal Hospital Baselland, Liestal, Switzerland*
[3]*Cardiology, University Hospital Basel, University of Basel, Basel, Switzerland*
[4]*Cardiology, Cantonal Hospital Baselland, Liestal, Switzerland*

**Correspondence to: Katharina Glatz, Pathology, Institute of Medical Genetics and Pathology, University Hospital Basel, University of Basel, Schönbeinstrasse 40, CH-4031 Basel, Switzerland. E-mail: kathrin.glatz@usb.ch*

Abstract

While coronavirus disease 2019 (COVID-19) primarily affects the respiratory tract, pathophysiological changes of the cardiovascular system remain to be elucidated. We performed a retrospective cardiopathological analysis of the heart and vasculature from 23 autopsies of COVID-19 patients, comparing the findings with control tissue. Myocardium from autopsies of COVID-19 patients was categorised into severe acute respiratory syndrome coronavirus 2 (SARS-CoV-2) positive (n = 14) or negative (n = 9) based on the presence of viral RNA as determined by reverse transcriptase polymerase chain reaction (RT-PCR). Control tissue was selected from autopsies without COVID-19 (n = 10) with similar clinical sequelae. Histological characteristics were scored by ordinal and/or categorical grading. Five RT-PCR-positive cases underwent *in situ* hybridisation (ISH) for SARS-CoV-2. Patients with lethal COVID-19 infection were mostly male (78%) and had a high incidence of hypertension (91%), coronary artery disease (61%), and diabetes mellitus (48%). Patients with positive myocardial RT-PCR died earlier after hospital admission (5 versus 12 days, $p < 0.001$) than patients with negative RT-PCR. An increased severity of fibrin deposition, capillary dilatation, and microhaemorrhage was observed in RT-PCR-positive myocardium than in negatives and controls, with a positive correlation amongst these factors All cases with increased cardioinflammatory infiltrate, without myocyte necrosis (n = 4) or with myocarditis (n = 1), were RT-PCR negative. ISH revealed positivity of viral RNA in interstitial cells. Myocardial capillary dilatation, fibrin deposition, and microhaemorrhage may be the histomorphological correlate of COVID-19-associated coagulopathy. Increased cardioinflammation including one case of myocarditis was only detected in RT-PCR-negative hearts with significantly longer hospitalisation time. This may imply a secondary immunological response warranting further characterisation.

Keywords: COVID-19; SARS-CoV-2; myocarditis; haemorrhagic diathesis; microangiopathy

Received 17 January 2021; Revised 23 February 2021; Accepted 10 March 2021

No conflicts of interest were declared.

Introduction

Coronavirus disease 2019 (COVID-19) caused by severe acute respiratory syndrome coronavirus 2 (SARS-CoV-2) has rapidly evolved into one of the most significant public health crises of the 21st century. While chiefly a respiratory disease, a wide spectrum of SARS-CoV-2-associated cardiovascular sequelae have been described in the literature. These include elevated cardiac troponins [1], associated with worse outcome and an increased mortality rate [2,3], heart failure [4], arrhythmias, bundle branch block, tachycardia–bradycardia syndrome, and/or non-specific repolarisation changes in electrocardiograms (ECG) [5] and occasional ST-segment elevation myocardial infarction [6,7]. Most notably, a higher mean age and incidence of cardiovascular risk factors and comorbidities such as hypertension, coronary heart disease, heart failure, obesity, diabetes mellitus, and cardiac amyloidosis have been observed in patients with severe disease [8,9].

SARS-CoV-2 utilises its spike (S) protein to bind to the membrane-bound form of angiotensin-converting enzyme 2 (ACE2) receptor [10]. The heart has been proposed as a potential direct target of viral entry, as ACE2 has been found to be expressed in cardiomyocytes, fibroblasts, endothelium, and pericytes [11,12]. Electron microscopy (EM) has detected SARS-CoV-2 both in the interstitial compartment of the myocardium [13,14] and occasionally in the cardiomyocytes themselves [15]; these findings were mirrored by *in situ* hybridisation (ISH) [12,16]. Recently performed *in vitro* studies demonstrated that SARS-CoV-2 was able to directly infect pluripotent stem cell-derived cardiomyocytes [17]. These data are strongly suggestive of a potential cardiotropic effect of SARS-CoV-2 which may contribute to the cardiovascular manifestations discussed above, although its mechanisms may be more complex than initially imagined and warrant further study.

Secondary dysregulation of the immune response in the form of a cytokine storm has been observed in COVID-19 [18]. Rapid viral replication leads to a disproportionate mobilisation of neutrophils, monocytes, and endothelial dysfunction leading to acute lung injury and multi-organ failure, including cardiac dysfunction [19]. An increased risk for thromboembolic events, likely due to microvascular dysfunction [20,21], has been observed in both clinical and autopsy series with severe or lethal outcome despite receipt of anticoagulation [9,22,23]. In addition, post-mortem investigations have proposed the development of global endothelialitis in lethal disease [24].

COVID-19-associated myocarditis has been delineated in several case studies. Clinical diagnosis was based on serology, ECG, echocardiography, and cardiac magnetic resonance [13,25–27]. However, histological findings varied, ranging from lymphocytic myocarditis without the presence of SARS-CoV-2 [28] to mild interstitial and endocardial inflammation without fulfilling diagnostic criteria [13]. A comparison between patients with increased versus insignificant myocardial viral load revealed no significant difference in inflammatory infiltrate [16]. Several potential pathophysiological mechanisms behind these findings have since been suggested, including direct viral injury, endothelialitis, interleukin (IL)-6-induced cytokine storm, and auto-antibodies [27], which calls for further studies characterising the cardiac inflammatory effects in COVID-19.

To further analyse the full spectrum of SARS-CoV-2-associated cardiopathy, we performed a systematic cardiopathological characterisation of lethal COVID-19 in 23 autopsies.

Materials and methods

Study design, cohort, and patient selection

Twenty-three autopsies of patients with COVID-19 were performed at the pathology departments of the University Hospital of Basel (n = 12) and the Cantonal Hospital Baselland, Liestal (n = 11), from March to June 2020. All decedents were diagnosed with COVID-19 as per antemortem nasopharyngeal swab. Full body autopsy was performed in 21 cases (91%); a partial autopsy of the upper respiratory tract, lungs, and heart (n = 2, 9%) was conducted in cases with excessive overweight or according to patient or relatives' wishes. In all 23 cases, the cause of death at autopsy was COVID-19-associated respiratory failure (by either acute respiratory distress syndrome/diffuse alveolar damage [ARDS/DAD], pulmonary embolism [PE], and/or bronchopneumonia). Myocardial reverse transcriptase polymerase chain reaction (RT-PCR) C_T values (cycle threshold) were utilised to classify cases into RT-PCR-positive (n = 15) and -negative (n = 8) subgroups. Autopsies without COVID-19 (n = 10) but with similar sequelae (ARDS/DAD n = 7; PE n = 2; bronchopneumonia n = 1) were selected as controls. The overall mean time to fixation was 29.14 h (5.3–84.5). Table 1 lists clinical features, comorbidities, pharmacology, laboratory results, and ECG findings of COVID-19 patients and controls. Angiotensin-converting enzyme inhibitors, angiotensin receptor blockers, renin inhibitors, and aldosterone inhibitors were defined as renin angiotensin aldosterone system (RAAS) inhibitors. Anticoagulants included heparin and its derivatives, new oral anticoagulants, coumarin derivatives, and/or platelet aggregation inhibitors. This study was approved by the Ethics Committee of Northwestern and Central Switzerland (ID 2020-00629).

Gross analysis of the heart and vasculature

All hearts and greater vessels were dissected in the direction of blood flow. The extent of coronary atherosclerosis, stenosis, aortic atherosclerosis, and atrial dilatation was recorded ordinally and/or nominally. Cardiac hypertrophy was determined by gender-dependent percentile curves according to body mass index (BMI) and heart weight (see Supplementary material for gross findings and scoring methodology).

Histological analysis

Representative tissue sections (0.4 × 1 × 2 cm) of the left anterior and posterior wall, the interventricular septum, and papillary muscles of the left ventricle and interventricular septum were extracted at autopsy and preserved in 4% phosphate-buffered formalin before being processed. In seven cases, a sample of the right

Table 1. Clinical characteristics of patients with positive and negative myocardial SARS-CoV-2 RT-PCR compared to controls.

	COVID-19 patients					
	Myocardial RT-PCR positive (n = 14)	Myocardial RT-PCR negative (n = 9)	All (n = 23)	Controls (n = 10)	Significance between RT-PCR positive, negative, and controls (P value)	Significance between COVID-19 patients and controls (P value)
General characteristics						
Sex, male (%)	13 (93)	5 (56)	18 (78)	8 (80)	0.11	0.65
Age, mean (SD)	79 (12)	70 (12)	76 (13)	64 (14)	**0.02**	**0.01**
BMI, median (IQR)	27 (26–29)	30 (27–41)	27 (26–35)	23 (22–31)	0.12	0.07
Hospitalisation, median days (IQR)	5 (3–7)	12 (9–33)	7 (5–12)	7 (6–30)	**0.005**	0.48
ICU admission (%)	4 (29)	3 (33)	7 (30)	6 (60)	0.32	0.11
ECMO (%)	0 (0)	1 (11)	1 (4)	1 (10)	0.32	0.52
Mechanical ventilation (%)	3 (21)	3 (33)	6 (26)	3 (30)	0.79	0.57
Initial presentation						
Cough	10 (71)	9 (100)	19 (83)	0 (0)	**<0.001**	**<0.001**
Dyspnoea	8 (57)	3 (33)	11 (48)	7 (70)	0.33	0.21
Fever	6 (43)	9 (100)	15 (65)	2 (20)	**0.001**	**0.02**
Comorbidities						
Hypertension (%)	14 (100)	7 (78)	21 (91)	7 (70)	**<0.001**	**0.001**
Cardiovascular disease (%)	10 (71)	4 (44)	14 (61)	2 (20)	0.05	**0.04**
COPD (%)	2 (14)	2 (22)	4 (17)	1 (10)	0.85	0.52
Diabetes mellitus (%)	6 (43)	5 (56)	11 (48)	1 (10)	0.12	**0.04**
Pharmacology						
Before admission						
RAAS inhibitors (%)	10 (71)	2 (22)	12 (52)	3 (30)	**0.04**	0.21
Anticoagulation and/or platelet aggregation inhibition (%)	9 (64)	6 (67)	15 (65)	2 (20)	0.10	**0.04**
During hospitalisation						
Anticoagulation and/or platelet aggregation inhibition (%)	14 (100)	8 (89)	22 (96)	5 (50)	**0.02**	**0.004**
Hydroxy-chloroquine (%)	10 (71)	4 (44)	14 (61)	0 (0)	**0.001**	**0.001**
Tocilizumab (%)	4 (29)	1 (11)	5 (22)	0 (0)	0.15	0.14
Laboratory results (last available before exitus)						
CRP, mg/dl, median (IQR)	199 (113–337)	166.9 (100–280)	176 (121–271)	56 (14–159)	0.09	**0.03**
Haemoglobin, g/l, median (IQR)	106 (95–129)	113 (96–122)	109 (97–126)	83 (82–125)	0.05	**0.01**
Leucocytes (10^{-9}/l), median (IQR)	10.0 (7.4–16.0)	8.1 (6.3–13.8)	8.8 (7.4–12.4)	9.4 (2.4–15.7)	0.82	0.92
Lymphocytes (10^{-9}/l), median (IQR)	0.5 (0.4–0.7)	0.9 (0.4–1.5)	0.61 (0.4–0.96)	7.7 (0.8–13.3)	**0.02**	**<0.01**
Neutrophilic granulocytes (10^{-9}/l), median (IQR)	7.4 (6.6–10.9)	6.2 (3.3–7.3)	6.8 (6.1–10.1)	54.8 (15.7–82.8)	**0.003**	**<0.01**
Thrombocytes ($10^{-9/}$l), median (IQR)	160 (109–331)	98 (53–400)	126 (104–225)	89 (70–409)	0.74	0.76
INR, median (IQR)	1.3 (1.2–1.9)	1.2 (1.2–1.4)	1.3 (1.2–1.7)	1.2 (1.2–1.8)	0.66	0.71
LDH, median (U/l)	444 (321–1605)	663 (654–1635)	628 (321–753)	434 (269–1175)	0.53	0.34
Creatinine (µg/l), median (IQR)	291 (120–706)	70 (47–192)	133 (84–407)	177 (59–243)	0.09	0.72

Values in bold indicate significant P values at the 0.05 level.
COPD, chronic obstructive pulmonary disease; CRP, C-reactive protein; ECMO, extracorporeal membrane oxygenation; ICU, intensive care unit; INR, international normalised ratio; IQR, interquartile range; LDH, lactate dehydrogenase; SD, standard deviation.

ventricle was extracted. Standard histological staining protocols (haematoxylin and eosin [H&E] and chromotrope aniline blue [CAB]) were applied. In cases with suspected cardiac amyloidosis, Congo red staining was performed. In addition, immunohistochemical staining of fibrin, cluster of differentiation (CD) 3, CD68, ACE2, κ and λ immunoglobulin light chains, antisera to amyloid A, and transthyretin (ATTR) for amyloid subtyping was performed in line with previously described protocols [29,30]. Immunohistochemical detection of ACE2 (Abcam ab15348, polyclonal, rabbit, 1:10,000) (ABCAM, Cambridge, UK) and staining for viral nucleocapsid (N)-protein (Rockland #200-401-A50, polyclonal, rabbit, 1:2,000) (Rockland Immunochemicals Inc, Limerick, PA, USA) was performed in all COVID-19 cases. Histomorphological characteristics, such as hypertrophy, ischaemic changes (contraction band necroses/

infarction), oedema, fibrosis, amyloidosis, capillary/arteriolar fibrin deposition, and erythrocyte anisocytosis, were graded with ordinal, nominal, and/or categorical scales (see Supplementary material for full details on histological scoring).

Increased numbers of intravascular granulocytes and mononuclear cells and intramyocardial lymphohistiocytic inflammatory infiltrates outside of areas of fibrosis and unassociated with tissue repair were assessed on H&E. Intramyocardial inflammatory cells were additionally quantified by immunohistochemistry (IHC; CD3-, CD20-, and CD68-positive cells/mm^2). Seven or fewer (≤7) single CD3-positive T-lymphocytes/mm^2 and 3 or fewer (≤3) single CD68-positive histiocytes outside areas of fibrosis were considered physiological. Increased cardioinflammatory infiltrate without necrosis was defined by the presence of clusters (≥3 CD3-positive T-lymphocytes in non-fibrotic myocardium) and foci (≥14 leucocytic cells/mm^2 including ≤4 monocytes/mm^2 and ≥7 CD3-positive T-lymphocytes/mm^2). Myocarditis was defined as increased cardioinflammatory infiltrate with associated cardiomyocyte necrosis.

The histomorphological distribution of ACE2 expression in stromal and endothelial cells was assessed qualitatively. ACE2-positive epicardial fat cells served as a positive internal control.

Ancillary techniques

For a detailed description of RT-PCR, ISH, and EM protocols, see Supplementary material.

Statistical analysis

Statistical analyses were performed using IBM® SPSS® Statistics, Version 25.0 (2017) (Armonk, NY, USA). Significance testing was performed between three groups (RT-PCR positive, RT-PCR negative, and controls) and two groups (COVID-19 patients and controls). In parametric data sets, a one-way analysis of variance (ANOVA) and an independent sample *t*-test were performed. For non-parametric or ordinal variables, Kruskal–Wallis one-way ANOVA and Mann Whitney *U*-test were used. Appropriate *post hoc* testing was subsequently performed on all statistically significant variables with more than two groups (Tukey's honestly significant difference for parametric and Dunn's test for non-parametric variables; see Supplementary material for all values). A two-tailed Fisher's exact test was performed for categorical variables. Correlation analyses of myocardial characteristics was performed using Spearman's rank-order correlation. Pearson's correlation was utilised to correlate viral copy numbers between the lung and myocardium (see Supplementary material). *P* values were considered significant at the 0.05 level.

Results

Clinical characteristics

Clinical characteristics are displayed in Table 1. The median BMI was 27 and 78% were male. Amongst COVID-19 patients, myocardial RT-PCR-negative cases experienced longer hospitalisation times than positive cases (12 versus 5 days; $p < 0.005$). COVID-19 patients had a significantly higher mean age (76 versus 64 years; $p = 0.01$) than controls. Hypertension (91 versus 70%; $p < 0.001$) and a history or current diagnosis of coronary artery disease (61 versus 20%; $p = 0.04$) and diabetes mellitus (48 versus 10%; $p = 0.04$) were more common amongst COVID-19 patients compared to controls. An intake of RAAS inhibitors was more likely amongst myocardial RT-PCR-positive patients than negatives or controls (71 versus 22 versus 30%; $p = 0.04$). Intake of anticoagulants and/or platelet aggregation inhibitors before and during hospital admission was more common amongst COVID-19 patients than controls (before: 65 versus 20%, $p = 0.04$; during: 96 versus 50%,

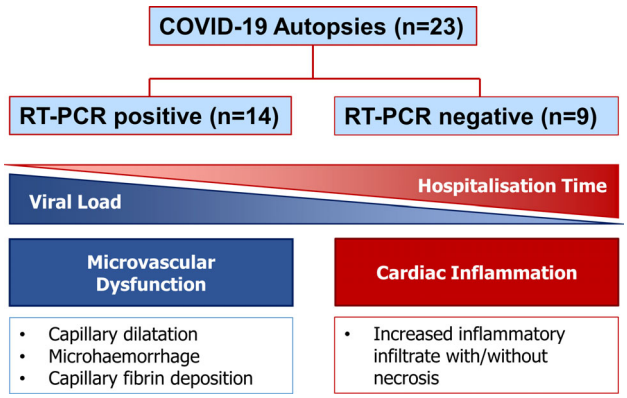

Figure 1. Temporal evolution of COVID-19-associated cardiopathy: early microvasculopathy followed by secondary cardioinflammatory response. Myocardium from autopsies of COVID-19 patients ($n = 23$) was classified based on SARS-CoV-2 presence determined by RT-PCR. Cases with detectable viral loads (RT-PCR positive) displayed higher severity of capillary dilatation, fibrin deposition, and microhaemorrhage, a histomorphological correlate of microvascular dysfunction. In RT-PCR-negative cases ($n = 9$), a high incidence of predominantly subtle cardioinflammatory pathologies was observed (including one case with lymphohistiocytic myocarditis), along with a longer hospitalisation time.

$p = 0.004$). Most recently available laboratory findings before death revealed significantly higher C-reactive protein (176.4 versus 56 mg/dl; $p = 0.03$) in COVID-19 patients versus controls. Leucocyte differentiation showed severe lymphopenia (median: 0.61×10^{-9}/l) and mild neutrophilia (median: 6.8×10^{-9}/l) in COVID-19 patients. High-sensitivity troponin T (hs-troponin T) was measured in eight (34%) COVID-19 patients; its median value in RT-PCR-positive and -negative cases was 77 and 98 ng/l, respectively.

Table 2. Histological findings of patients with positive and negative SARS-CoV-2 RT-PCR compared to controls.

	COVID-19 patients					
	Myocardial RT-PCR positive ($n = 14$)	Myocardial RT-PCR negative ($n = 9$)	All ($n = 23$)	Controls ($n = 10$)	Significance between RT-PCR positive, negative, and controls (P value)	Significance between COVID-19 patients and controls (P value)
Hypertrophy (%)					0.08	0.06
None	1 (7)	1 (11)	2 (9)	2 (20)		
Mild	7 (50)	5 (56)	12 (52)	8 (80)		
Marked	6 (43)	3 (33)	9 (39)	0 (0)		
Overall	13 (93)	8 (89)	21 (91)	8 (80)		
Fibrosis (%)					0.50	0.32
None	1 (7)	2 (22)	3 (13)	4 (40)		
Interstitial	7 (50)	5 (56)	12 (52)	5 (50)		
Replacement	4 (29)	1 (11)	5 (22)	1 (10)		
Infarct scar	2 (14)	1 (11)	3 (13)	0 (0)		
Overall	13 (93)	7 (78)	20 (87)	6 (60)		
Ischaemic necrosis (%)					0.20	0.70
Contraction band necroses	3 (21)	3 (33)	6 (26)	1 (10)		
Infarction	0 (0)	1 (11)	1 (4)	1 (10)		
Overall	3 (21)	4 (45)	7 (30)	2 (20)		
Amyloidosis (%)					0.19	0.45
0% of tissue	9 (64)	8 (89)	17 (74)	9 (90)		
1–29% of tissue	3 (21)	1 (11)	4 (17)	1 (10)		
≥30% of tissue	2 (14)	0 (0)	2 (9)	0 (0)		
Overall	5 (36)	1 (11)	6 (26)	1 (10)		
Capillary dilatation (%)					**0.04**	0.13
None	0 (0)	1 (11)	1 (4)	1 (10)		
Mild	5 (36)	6 (67)	11 (48)	7 (70)		
Marked	9 (64)	2 (22)	11 (48)	2 (20)		
Overall	14 (100)	8 (89)	22 (96)	9 (90)		
Microhaemorrhage (%)					**0.03**	**0.04**
None	5 (36)	5 (56)	10 (43)	9 (10)		
Focal	6 (43)	2 (22)	8 (35)	1 (10)		
Extensive	3 (21)	2 (22)	5 (22)	0 (0)		
Overall	9 (64)	4 (45)	13 (57)	1 (10)		
Capillary fibrin (%)					**0.04**	**0.04**
None	0 (0)	0 (0)	0 (0)	3 (30)		
Focal	8 (57)	7 (78)	15 (65)	6 (60)		
Extensive	6 (64)	2 (22)	8 (35)	1 (10)		
Overall	14 (100)	9 (100)	23 (100)	7 (70)		
Arteriolar fibrin (%)	2 (14)	3 (33)	5 (22)	1 (10)	0.45	0.64
Anisocytosis of intravascular erythrocytes (%)	9 (64)	5 (56)	14 (61)	9 (90)	0.28	0.32
Inflammation						
Interstitial oedema (%)	7 (50)	8 (89)	15 (65)	6 (60)	0.18	0.54
Increased myocardial CD68-positive cells	3 (21)	6 (67)	9 (39)	2 (20)	0.06	0.26
Cardioinflammation						
Increased infiltrate without necrosis	0 (0)	4 (44)	4 (17)	1 (10)	**0.007**	0.52
Lymphohistiocytic myocarditis	0 (0)	1 (11)	1 (4)	0 (0)	0.27	0.70
Overall	0 (0)	5 (56)	5 (22)	1 (10)	**0.001**	0.64

Values in bold indicate significant P values at the 0.05 level.
IQR, interquartile range.

General post-mortem findings

A graphical overview of histological findings can be found in Figure 1. Gross findings are summarised in Table 2. Heart weight ranged from 430 to 550 g amongst COVID-19 patients (median: 468 g). There was a significantly higher incidence of predominantly eccentric hypertrophy amongst RT-PCR-positive hearts (93%) compared to RT-PCR negatives (67%) or controls (60%; $p = 0.04$). Thirteen percent of COVID-19 cases presented with coronary stenosis. Histological analysis of fibrotic changes revealed no difference between categories (interstitial, replacement, and infarct scar) when comparing COVID-19 cases to controls. Small foci of non-territorial myocyte necroses were observed in 26% of COVID-19 patients, and one case (4%) presented with acute transmural type 1 myocardial infarction of the anterior and lateral wall of the left ventricle (diameter: 7 cm) with perforation and fatal pericardial tamponade (Figure 2). Analysis of coronary vessels revealed an acute thrombotic occlusion of the left anterior descending artery as the cause of infarction. Histological analysis of the right ventricle in 7 of 23 cases revealed unremarkable findings devoid of right heart dilatation and/or stress; none of the samples showed contraction band necroses.

Detection of SARS-CoV-2 in the myocardium and correlation between myocardial and pulmonary viral load

RT-PCR of COVID-19 patients revealed positive C_T values in 14 (61%) out of 23 cases. Myocardial SARS-CoV-2 genomes/10^6 RNase-P copies correlated significantly with values measured in lung tissue of the same cohort (Pearson correlation between myocardial and pulmonary SARS-CoV-2 genomes/10^6 RNase-P copies: $r = 0.622$; $p = 0.001$). Pulmonary viral load was significantly higher in the lungs than in the myocardium ($p = 0.0057$, Student's t-test) and there were no cases of isolated myocardial positivity (see Supplementary material). IHC for N-protein and ISH revealed scarce positivity in interstitial cells without detection in cardiomyocytes (Figure 3). EM performed in two RT-PCR-positive cases did not detect viral particles in cardiomyocytes or interstitial cells.

Myocardial microvascular changes

An overview of microvascular histology findings is displayed in Figure 4. While its incidence did not differ between groups, the distribution of capillary dilatation

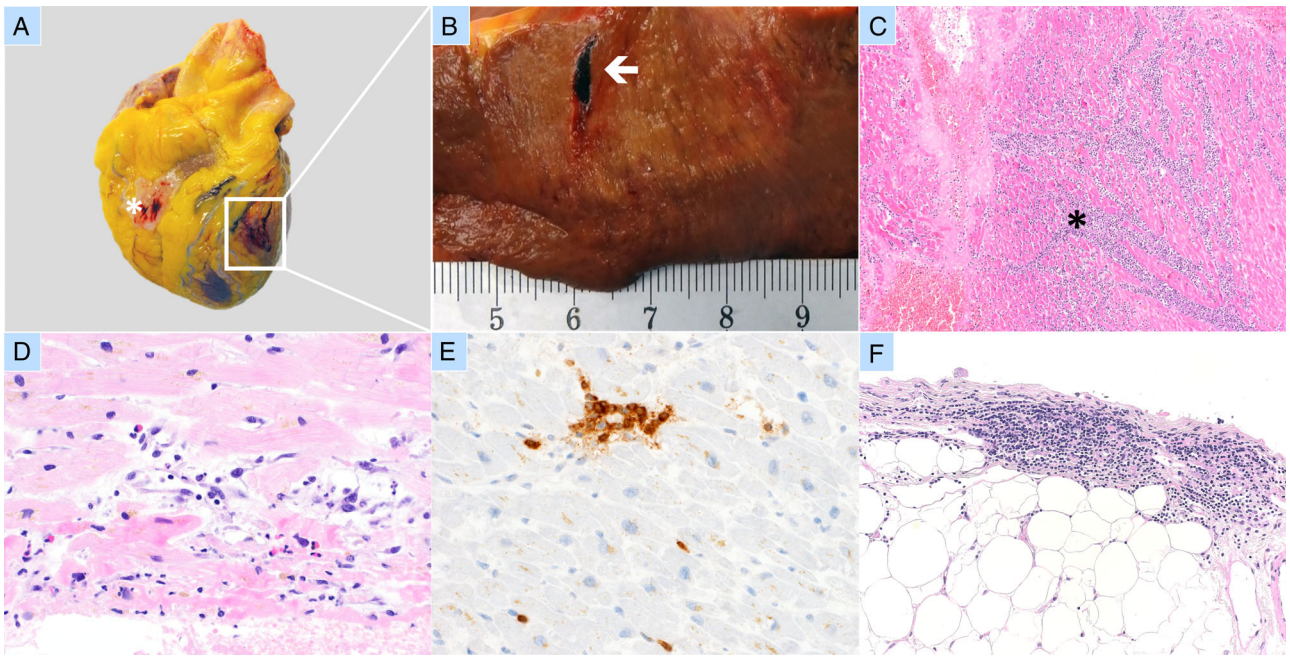

Figure 2. Independently occurring concurrent active lymphohistiocytic perimyocarditis and acute myocardial infarction with transmural perforation in a case of lethal COVID-19. (A–C) Acute myocardial infarction. (A) Gross findings – haemorrhagic diathesis of epicardium (*); transmural perforation of the anterior myocardial wall (white box). (B) Close-up view of perforation (white arrow) with gross signs of acute infarction (territorial parenchymal pallor and yellowish discolouration). (C) Acute myocardial infarction in the region of perforation with territorial coagulation necrosis and dense infiltrates of neutrophilic granulocytes (black asterisk). (D–F) Active lymphohistiocytic myocarditis. (D) Lymphohistiocytic infiltrates and few eosinophils associated with necrotic hypereosinophilic cardiomyocytes with contraction bands; (E) cluster of T-lymphocytes (CD3 IHC, ×400); (F) lymphocytic infiltrate in the epicardial fat.

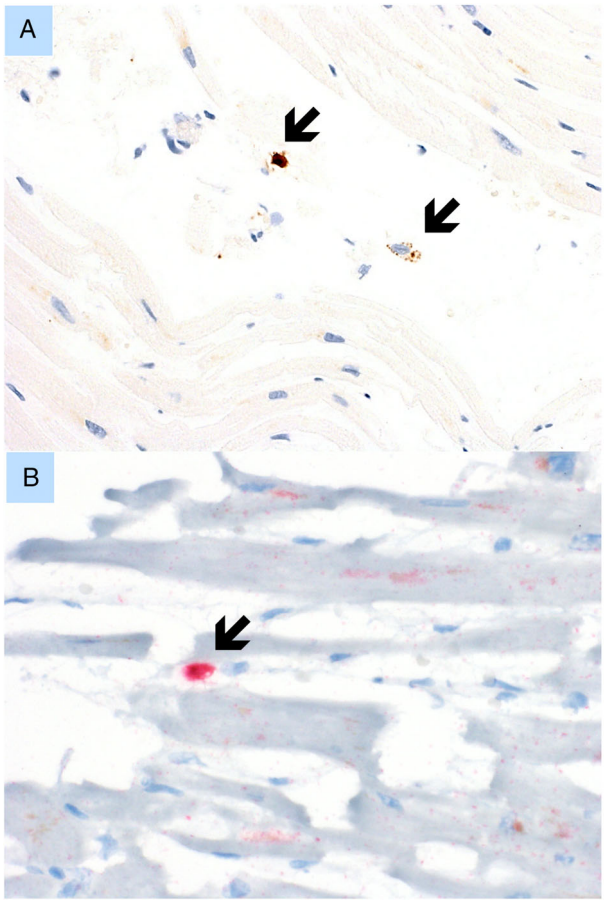

Figure 3. Detection of SARS-CoV-2 in the myocardium. (A) Deposits of N-protein in interstitial cells of likely monocytic origin (black arrows) (N-protein IHC, ×400). (B) Open reading frame ab1- and S-RNA ISH reveal isolated positivity in the interstitium (black arrow) (ISH, ×400).

varied significantly between RT-PCR positives, negatives, and controls ($p = 0.04$) – it was particularly severe in RT-PCR-positive myocardium (64% marked) compared to negatives (22% marked). The overall incidence of marked capillary dilatation was 48% in COVID-19 patients versus 20% in controls. An overall higher incidence of both focal (35%) and extensive (22%) microhaemorrhages was observed in COVID-19 patients versus controls, which also yielded a statistically significant difference in distribution (RT-PCR positive versus negative versus controls: $p = 0.03$; COVID-19 versus controls: $p = 0.04$). All COVID-19 cases manifested capillary fibrin deposition; a significant difference in its distribution was observed between all groups ($p = 0.04$) and between COVID-19 patients and controls ($p = 0.04$); 64% of RT-PCR-positive myocardium presented with extensive deposition versus 22% of RT-PCR negatives. There were significant positive correlations between capillary dilatation, microhaemorrhage, and capillary fibrin deposition (capillary dilatation–microhaemorrhage: $\rho = 0.61$, $p < 0.01$; capillary dilatation–capillary fibrin: $\rho = 0.36$, $p = 0.04$; capillary fibrin–microhaemorrhage: $\rho = 0.35$, $p = 0.04$).

In lieu with fibrin deposition, erythrocyte deformation and anisocytosis in capillaries were observed in 61% of COVID-19 patients. The myocardial capillaries of two COVID-19 patients examined by EM contained densely packed, fragmented, and deformed erythrocytes coated with a thin layer of fibrin and extensive filamentous fibrin deposits along capillary walls (Figure 4C). In areas of haemorrhage, capillaries were replete with erythrocytes presenting with focal wall ruptures. However, no statistically significant incidence of erythrocyte anisocytosis was observed compared to controls.

Six patients (26%) with COVID-19 presented with cardiac amyloidosis, which in all cases was immunohistochemically subtyped as senile ATTR amyloidosis.

Inflammatory changes

Increased numbers of interstitial CD68-positive macrophages were observed in COVID-19 patients compared to controls (39 versus 20%; 67% of RT-PCR-negative cases). A total of four COVID-19 cases (17%) presented with an increased lymphohistiocytic infiltrate without the presence of myocyte necrosis. In one case (4%), both active lymphohistiocytic myocarditis without fibrosis characterised by several active, necrotising inflammatory foci and an acute transmural infarction resulting in lethal perforation of the myocardial wall with associated ischaemic inflammation in a different locus were observed (Figure 2). All cases with increased cardioinflammatory infiltrate were RT-PCR negative. Only one case in the control group exhibited histological signs of increased cardioinflammation without necrosis (10%).

Angiotensin-converting enzyme 2

Myocardial ACE2 was detected in stromal cells with either granular cytoplasmic and/or membranous positivity. No notable differences in staining patterns between COVID-19 patients and controls were observed.

Discussion

Correlation between clinical and post-mortem findings

In this study, we assessed cardiopathological characteristics in 23 lethal cases of COVID-19. The

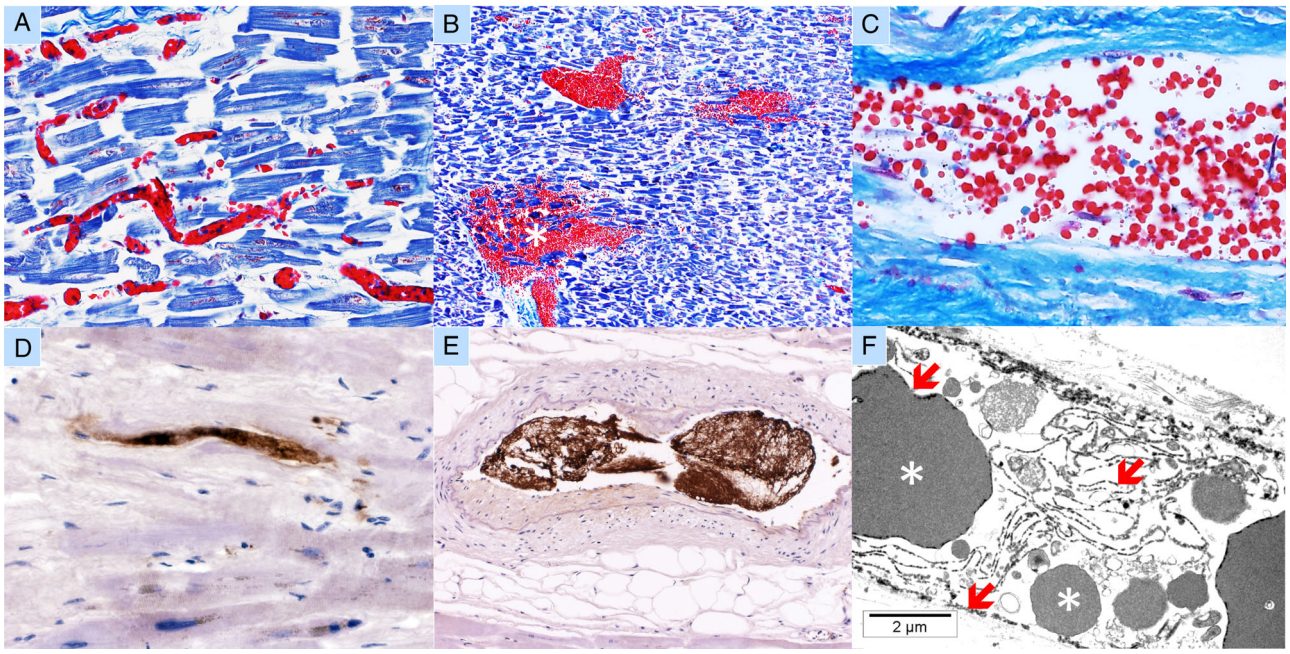

Figure 4. Myocardial microvascular dysfunction in lethal COVID-19. (A) Marked capillary dilatation (CAB, ×400). (B) Hyperaemic vessels with parenchymal microhaemorrhage (*) (CAB, ×100). (C) Intraluminal erythrocyte anisocytosis (CAB, ×400). (D) Fibrin thrombus in an intramyocardial capillary (fibrin IHC, ×400). (E) Arterial fibrin thrombus (fibrin IHC, ×200). (F) Capillary vessel containing anisocytotic erythrocytes, a thin coat of fibrin on erythrocytes, vessel wall, and intraluminal fibrin threads (red arrows) (EM).

incidence of hypertension, coronary artery disease, and diabetes mellitus was high amongst COVID-19 patients, in line with the high incidence of cardiovascular comorbidities in patients with lethal COVID-19 that has repeatedly been shown in the literature [4,8]. Our findings mirror a meta-analysis of comorbidity prevalence of seven clinical studies, which reported pooled odds ratios of 2.36 for hypertension and 3.42 for cardiovascular disease between mild and severe disease outcome [31], thus further underlining the critical role of cardiovascular comorbidities in the pathogenesis of severe COVID-19. This is further supported by a high incidence of eccentric hypertrophy amongst COVID-19 patients (78%; Table 2), which is considered as long-term adaptation to hypertension and may thus be a predisposing factor for severe disease. A complex relationship between cardiovascular risk factors and immune response [32,33], as well as a potential role of immunosenescence [34] are all plausible pathophysiological explanations behind these observations. Identification of these patient subgroups should therefore play an instrumental role in risk stratification for early therapeutic intervention.

Detection of SARS-CoV-2 in the myocardium

Sixty percent of cases in this cohort (14/23) displayed myocardial RT-PCR positivity by SARS-CoV-2 PCR. It however remains to be elucidated whether this finding is a reflection of parenchymal viral load or merely due to packaged virions in contaminated blood. A significant positive correlation with the viral load in lungs (see Supplementary material) seems to support the latter, although ancillary techniques (IHC against the N-protein, ISH, and EM) did not detect viral presence in cardiomyocytes in this study. A broad array of studies have detected viral presence in both interstitial compartments and occasionally in cardiomyocytes [12,13,15,16], although data are presently sporadic and do not exclude a potential cardiotropic nature of SARS-CoV-2.

Myocardial microvascular dysfunction

Histomorphological analysis of the myocardium in COVID-19 patients revealed significantly higher levels of capillary fibrin deposition, capillary dilatation, and parenchymal microhaemorrhages compared with 10 autopsies without SARS-CoV-2 infection but similar sequelae. These morphological alterations of the microvasculature correlated positively amongst each

other, suggesting potential causality and also suggesting a myocardial manifestation of the hypercoagulable state in severe COVID-19 in the form of microangiopathic disease. We postulate that capillary fibrin deposition causes microcirculatory stasis, resulting in focal microhaemorrhages due to increased intravascular pressure and permeability of the endothelial barrier [35]. Erythrocyte anisocytosis in capillary lumina, detected on both light microscopy and EM, further supports these findings as a possible histomorphological correlate of disseminated intravascular coagulation and complement activation. Our initial post-mortem series analysing the same cohort parallels these observations, reporting an increased incidence of pulmonary microthrombi indicative of vascular dysfunction [9]. Another autopsy case series observed a systemic incidence of microthrombi in the microvasculature of several organ systems including the heart, thus confirming the systemic nature of COVID-19-associated microvasculopathy [36]. Our results are similarly in line with clinical observations which report an increased incidence of thromboembolic events in severe COVID-19 [22,37]. Remarkably, no necroses associated with the microhaemorrhages were histologically detectable. It therefore remains questionable whether these microangiopathic changes have a significant impact on myocardial function. In our cohort, senile cardiac ATTR amyloidosis amongst COVID-19 patients (26%) was more common than its incidence amongst autopsies performed in Basel between 2018 and 2019 [9]. These findings may be relevant, as cardiac amyloidosis has previously been reported to impact microvascular dysfunction [38], purportedly predisposing to the aforementioned observations in COVID-19 vasculopathy.

Myocardial ischaemia

As denoted in previous observational studies, acute coronary syndrome can be triggered by COVID-19 and even be its primary symptom [7]. Possible pathophysiological explanations of angina pectoris in COVID-19 include plaque rupture, occlusive thrombosis, or coronary spasm [39]. In our study, ECG of COVID-19 patients did not reveal significant or specific changes related to ischaemic events, although non-specific conduction and/or repolarisation abnormalities were reported (Table 1). Furthermore, only one case of acute territorial transmural infarction in conjunction with pericardial tamponade was observed amongst COVID-19 patients (Figure 2). In this case, we believe that the infarction, caused by thrombotic occlusion of the left anterior descending artery, was solely responsible for the wall rupture despite concurrently diagnosed active myocarditis. Moreover, infrequent small foci of acute and subacute non-territorial ischaemic necroses in 17% of COVID-19 patients did not statistically differ from controls, mirroring previous findings [14]. Small foci of myocardial necrosis can occur due to a broad spectrum of aetiologies and are a frequent incidental post-mortem finding irrespective of the cause of death. Taken together, these findings suggest that ischaemic events are an uncommon observation in this cohort, although more extensive post-mortem series are needed for further characterisation.

Cardioinflammation

Four out of five cases with increased cardioinflammatory infiltrate presented without cardiomyocyte necrosis (n = 4) while one case presented as active, lymphohistiocytic myocarditis. These findings are in line with a literature review assessing the autopsy incidence of SARS-CoV-2-associated myocarditis, confirming that clinically relevant cardioinflammatory changes are generally a rare finding in COVID-19 [40,41]. Of note, all these cases were deemed RT-PCR negative. This finding is highly relevant when considering increased hospitalisation time amongst RT-PCR-negative patients, as it seems to mirror the behaviour of other types of viral myocarditis such as Coxsackie, citing infection as a precursor to delayed-onset cardiac inflammation in a complex, sequential cytokine response model [42]. Whether the myocardial effects observed in our study occur as a consequence of a systemic cytokine storm, are induced by auto-antibodies, or are the result of direct virally mediated injury remain to be elucidated. Lindner *et al* performed a cytokine gene expression panel on the myocardium of COVID-19 patients, noting that cases with increased viral load present with higher expression of tumour necrosis factor-α, interferon-γ, CCL5, IL-6, IL-8, and IL-18 [16]; however, the unique myocardial cytokine signature in response to COVID-19 is still unclear and the subject of ongoing studies. An increased influx of CD68-positive macrophages in 39% of COVID-19 patients, more prominently in RT-PCR-negative cases (75%), observed in our study is consistent with results from previous post-mortem reports [13,43]. This is supported by findings of ISH and N-protein IHC conducted in this study which revealed positivity in interstitial cells of likely monocytic origin (Figure 3B).

ACE2 and COVID-19

The role of ACE2 as a mediator of COVID-19-associated cardiopathy remains unclear. In our study, immunohistochemical analysis of ACE2 predominantly revealed positivity in stromal cells, in line with previous

gene expression analyses of myocardial ACE2 [10,12]. However, staining patterns did not markedly differ in control tissue. This contradicts a previously conducted investigation in SARS patients which observed weaker staining in patients versus controls, also denoting a significant decrease in ACE2 expression amongst SARS patients [44]. Notwithstanding these observations, the evaluation of immunohistochemical staining intensity and viability of RNA in post-mortem tissue varies with the extent of autolysis. Future studies are required to systematically study the basic biology of RAAS metabolites to shed light on the potential cardiotropic nature of SARS-CoV-2 and the role pharmacological inhibition of RAAS inhibitors may have on COVID-19 susceptibility.

Evidence of a biphasic disease progression in COVID-19 cardiac pathophysiology

One of the key observations of this study was significantly longer hospitalisation times (12 versus 5 days; $p = 0.005$) amongst myocardial RT-PCR-negative cases. This may either be because of a more serious disease progression in cases with higher myocardial viral load, leading to more rapid death, or due to gradual viral elimination as the disease progresses. The latter was suggested in a differential gene expression analysis conducted on the lungs of the same autopsy cohort, which identified two distinct immunopathological profiles based on interferon-stimulated gene (ISG) expression: ISG_{high} cases were identified as having an upregulation of ISGs, high viral load, and minimal pulmonary damage, while ISG_{low} cases featured downregulated ISGs, lower viral loads, and more extensive pulmonary damage with signs of remodelling [45]. Significantly longer hospitalisation times were observed in ISG_{low} cases. As all three genomic targets of myocardial RT-PCR viral load show significant positive correlation to pulmonary values (see Supplementary material), we postulate that there is some degree of concordance between the immunopathological profiles and the subgroups denoted in our study. A biphasic dynamic of COVID-19 progression may similarly be prevalent in the myocardium; microvascular changes, such as capillary dilatation, microhaemorrhage, and capillary fibrin deposition, show decrease in severity when comparing RT-PCR positive with negative cases (marked capillary dilatation: 64 to 22%; incidence of microhaemorrhage: 64 to 45%; extensive capillary fibrin: 64 to 22%), implying a dominance of microvascular pathology in early COVID-19 (Figure 1). Conversely, the extent of CD68-positive infiltrate (67 versus 21%) and the overall incidence of myocarditis are increased (22 versus 0%) in RT-PCR-negative cases compared to positives. Interestingly, ISG_{low} cases were also associated with increased presence of pulmonary $CD68^+$ macrophages, insinuating a migration from the lung to the myocardium in later stages of the disease. When comparing these trends with differential blood counts, an overall improvement of leucopenia (0.5 to 1.0×10^{-9}/l) and decrease of neutrophilia (7.4 to 6.1×10^{-9}/l) towards normal values further support our hypothesis that RT-PCR-positive and -negative subgroups represent a temporal evolution profile of immune viral response in COVID-19.

Methodological limitations

This study has several limitations. Its retrospective design resulted in inconsistent clinical data acquisition, such as missing hs-troponin T and N-terminal pro-brain natriuretic peptide values, in more than half of the data set. Moreover, the selection of controls as cases with COVID-19 suggestive sequelae was a challenge and may display several confounding factors; for instance, controls were significantly younger and presented with a high incidence of intensive care unit admission which may impact cardiac histomorphology. Moreover, the utilisation of ordinal scales in most histological analyses may comport limitations of statistical power in this study. In addition, there are currently no systematic data on assay sensitivity of SARS-CoV-2 RT-PCR in formalin-fixed, paraffin-embedded (FFPE) tissue, although consistency between ante-mortem swabs has been established in all our cases [9] and recent studies have been able to detect viral load in FFPE even in subclinical patients [46,47]; nonetheless, assay standardisation studies are required for both RT-PCR as well as other ancillary techniques for the detection of SARS-CoV-2 in FFPE tissue. Lastly, due to their mostly subtle manifestation, it is questionable whether the cardioinflammatory changes identified in this study would have been detected in an endomyocardial biopsy; in fact, small inflammatory foci without necrosis have previously been suggested be a non-specific finding at autopsy [48].

In conclusion, this cardiopathological study of myocardium in COVID-19 patients confirms a systemic manifestation of the SARS-CoV-2 hypercoagulable state extending to the myocardium, as well as an occurrence of subtle cardioinflammatory conditions in a subset of patients with longer hospitalisation duration and without detectable myocardial viral load.

Acknowledgements

The authors thank all patients included in this study and their relatives; Ralph Schoch and Thomas Rost for

assisting with dissection; PD Dr Thomas Menter, Dr Katharina Marston, Dr Fermin Person, Dr Daniel Turek, and Dr Simon Häfliger for conducting autopsies; and Susi Grieshaber, Petra Hirschmann, Valeria Perrina, Jan Schneeberger, and Martin Herzig for their expertise in IHC, ISH, RT-PCR, and EM. This study was funded by the Botnar Research Centre for Child Health.

Author contributions statement

JDH and KG wrote the manuscript, performed the gross and histological analyses and contributed the images. JDH, NS, KDM and AT performed autopsies. JDH, NS, RT and GL acquired clinical data. RN and AKS performed RT-PCR analysis and evaluation. JDH and RN performed the statistical analysis. AT, KDM, RT, GL, MM and NS carried out critical revision of the manuscript and discussion of the results.

References

1. Sandoval Y, Januzzi JL, Jaffe AS. Cardiac troponin for assessment of myocardial injury in COVID-19: JACC Review Topic of the Week. *J Am Coll Cardiol* 2020; **76:** 1244–1258.
2. Guo T, Fan Y, Chen M, *et al*. Cardiovascular implications of fatal outcomes of patients with coronavirus disease 2019 (COVID-19). *JAMA Cardiol* 2020; **5:** 811–818.
3. Shi S, Qin M, Shen B, *et al*. Association of cardiac injury with mortality in hospitalized patients with COVID-19 in Wuhan, China. *JAMA Cardiol* 2020; **5:** 802–810.
4. Chen T, Wu D, Chen H, *et al*. Clinical characteristics of 113 deceased patients with coronavirus disease 2019: retrospective study. *BMJ* 2020; **368**: m1091.
5. Angeli F, Spanevello A, De Ponti R, *et al*. Electrocardiographic features of patients with COVID-19 pneumonia. *Eur J Intern Med* 2020; **78:** 101–106.
6. Bangalore S, Sharma A, Slotwiner A, *et al*. ST-segment elevation in patients with Covid-19 – a case series. *N Engl J Med* 2020; **382:** 2478–2480.
7. Stefanini GG, Montorfano M, Trabattoni D, *et al*. ST-elevation myocardial infarction in patients with COVID-19: clinical and angiographic outcomes. *Circulation* 2020; **141:** 2113–2116.
8. Zhou F, Yu T, Du R, *et al*. Clinical course and risk factors for mortality of adult inpatients with COVID-19 in Wuhan, China: a retrospective cohort study. *Lancet* 2020; **395:** 1054–1062.
9. Menter T, Haslbauer JD, Nienhold R, *et al*. Post-mortem examination of COVID19 patients reveals diffuse alveolar damage with severe capillary congestion and variegated findings of lungs and other organs suggesting vascular dysfunction. *Histopathology* 2020; **77:** 198–209.
10. Nicin L, Abplanalp WT, Mellentin H, *et al*. Cell type-specific expression of the putative SARS-CoV-2 receptor ACE2 in human hearts. *Eur Heart J* 2020; **41:** 1804–1806.
11. Chen L, Li X, Chen M, *et al*. The ACE2 expression in human heart indicates new potential mechanism of heart injury among patients infected with SARS-CoV-2. *Cardiovasc Res* 2020; **116:** 1097–1100.
12. Sakamoto A, Kawakami R, Kawai K, *et al*. ACE2 (angiotensin-converting enzyme 2) and TMPRSS2 (transmembrane serine protease 2) expression and localization of SARS-CoV-2 infection in the human heart. *Arterioscler Thromb Vasc Biol* 2021; **41:** 542–544.
13. Tavazzi G, Pellegrini C, Maurelli M, *et al*. Myocardial localization of coronavirus in COVID-19 cardiogenic shock. *Eur J Heart Fail* 2020; **22:** 911–915.
14. Fox SE, Li G, Akmatbekov A, *et al*. Unexpected features of cardiac pathology in COVID-19 infection. *Circulation* 2020; **142:** 1123–1125.
15. Bulfamante GP, Perrucci GL, Falleni M, *et al*. Evidence of SARS-CoV-2 transcriptional activity in cardiomyocytes of COVID-19 patients without clinical signs of cardiac involvement. *Biomedicine* 2020; **8:** 626.
16. Lindner D, Fitzek A, Bräuninger H, *et al*. Association of cardiac infection with SARS-CoV-2 in confirmed COVID-19 autopsy cases. *JAMA Cardiol* 2020; **5:** 1281–1285.
17. Bojkova D, Wagner JUG, Shumliakivska M, *et al*. SARS-CoV-2 infects and induces cytotoxic effects in human cardiomyocytes. *Cardiovasc Res* 2020; **116:** 2207–2215.
18. Ragab D, Salah Eldin H, Taeimah M, *et al*. The COVID-19 cytokine storm; what we know so far. *Front Immunol* 2020; **11:** 1446.
19. Mann DL. Innate immunity and the failing heart: the cytokine hypothesis revisited. *Circ Res* 2015; **116:** 1254–1268.
20. Ackermann M, Verleden SE, Kuehnel M, *et al*. Pulmonary vascular endothelialitis, thrombosis, and angiogenesis in Covid-19. *N Engl J Med* 2020; **383:** 120–128.
21. Colantuoni A, Martini R, Caprari P, *et al*. COVID-19 sepsis and microcirculation dysfunction. *Front Physiol* 2020; **11:** 747.
22. Poissy J, Goutay J, Caplan M, *et al*. Pulmonary embolism in patients with COVID-19: awareness of an increased prevalence. *Circulation* 2020; **142:** 184–186.
23. Wichmann D, Sperhake J-P, Lütgehetmann M, *et al*. Autopsy findings and venous thromboembolism in patients with COVID-19: a prospective cohort study. *Ann Intern Med* 2020; **173:** 268–277.
24. Varga Z, Flammer AJ, Steiger P, *et al*. Endothelial cell infection and endotheliitis in COVID-19. *Lancet* 2020; **395:** 1417–1418.
25. Inciardi RM, Lupi L, Zaccone G, *et al*. Cardiac involvement in a patient with coronavirus disease 2019 (COVID-19). *JAMA Cardiol* 2020; **5:** 819–824.
26. Irabien-Ortiz Á, Carreras-Mora J, Sionis A, *et al*. Fulminant myocarditis due to COVID-19. *Rev Esp Cardiol (Engl Ed)* 2020; **73:** 503–504.
27. Van Linthout S, Klingel K, Tschöpe C. SARS-CoV-2-related myocarditis-like syndromes Shakespeare's question: what's in a name? *Eur J Heart Fail* 2020; **22:** 922–925.
28. Sala S, Peretto G, Gramegna M, *et al*. Acute myocarditis presenting as a reverse Tako-Tsubo syndrome in a patient with SARS-CoV-2 respiratory infection. *Eur Heart J* 2020; **41:** 1861–1862.
29. Menter T, Bachmann M, Grieshaber S, *et al*. A more accurate approach to amyloid detection and subtyping: combining in situ

Congo red staining and immunohistochemistry. *Pathobiology* 2017; **84:** 49–55.
30. Ehmann MA, Medinger M, Bodenmann B, *et al*. Histologic features of hematopoietic stem cell transplant-associated thrombotic microangiopathy are best percepted in deep skin biopsies and renal biopsies, while showing a significant overlap with changes related to severe acute graft-versus-host disease in gastrointestinal biopsies. *Bone Marrow Transplant* 2020; **55:** 1847–1850.
31. Yang J, Zheng Y, Gou X, *et al*. Prevalence of comorbidities and its effects in patients infected with SARS-CoV-2: a systematic review and meta-analysis. *Int J Infect Dis* 2020; **94:** 91–95.
32. Zhou T, Hu Z, Yang S, *et al*. Role of adaptive and innate immunity in type 2 diabetes mellitus. *J Diabetes Res* 2018; **2018:** 7457269.
33. Wenzel U, Turner JE, Krebs C, *et al*. Immune mechanisms in arterial hypertension. *J Am Soc Nephrol* 2016; **27:** 677–686.
34. Cunha LL, Perazzio SF, Azzi J, *et al*. Remodeling of the immune response with aging: immunosenescence and its potential impact on COVID-19 immune response. *Front Immunol* 2020; **11:** 1748.
35. Cardot-Leccia N, Hubiche T, Dellamonica J, *et al*. Pericyte alteration sheds light on micro-vasculopathy in COVID-19 infection. *Intensive Care Med* 2020; **46:** 1777–1778.
36. Rapkiewicz AV, Mai X, Carsons SE, *et al*. Megakaryocytes and platelet-fibrin thrombi characterize multi-organ thrombosis at autopsy in COVID-19: a case series. *EClinicalMedicine* 2020; **24:** 100434.
37. Artifoni M, Danic G, Gautier G, *et al*. Systematic assessment of venous thromboembolism in COVID-19 patients receiving thromboprophylaxis: incidence and role of D-dimer as predictive factors. *J Thromb Thrombolysis* 2020; **50:** 211–216.
38. Dorbala S, Vangala D, Bruyere J, *et al*. Coronary microvascular dysfunction is related to abnormalities in myocardial structure and function in cardiac amyloidosis. *JACC Heart Fail* 2014; **2:** 358–367.
39. Schiavone M, Gobbi C, Biondi-Zoccai G, *et al*. Acute coronary syndromes and Covid-19: exploring the uncertainties. *J Clin Med* 2020; **9:** 1683.
40. Halushka MK, Vander Heide RS. Myocarditis is rare in COVID-19 autopsies: cardiovascular findings across 277 postmortem examinations. *Cardiovasc Pathol* 2021; **50**: 107300.
41. Kawakami R, Sakamoto A, Kawai K, *et al*. Pathological evidence for SARS-CoV-2 as a cause of myocarditis. *J Am Coll Cardiol* 2021; **77:** 314–325.
42. Rose NR. Critical cytokine pathways to cardiac inflammation. *J Interferon Cytokine Res* 2011; **31:** 705–710.
43. Basso C, Leone O, Rizzo S, *et al*. Pathological features of COVID-19-associated myocardial injury: a multicentre cardiovascular pathology study. *Eur Heart J* 2020; **41:** 3827–3835.
44. Oudit GY, Kassiri Z, Jiang C, *et al*. SARS-coronavirus modulation of myocardial ACE2 expression and inflammation in patients with SARS. *Eur J Clin Invest* 2009; **39:** 618–625.
45. Nienhold R, Ciani Y, Koelzer VH, *et al*. Two distinct immunopathological profiles in autopsy lungs of COVID-19. *Nat Commun* 2020; **11:** 5086.
46. Guerini-Rocco E, Taormina SV, Vacirca D, *et al*. SARS-CoV-2 detection in formalin-fixed paraffin-embedded tissue specimens from surgical resection of tongue squamous cell carcinoma. *J Clin Pathol* 2020; **73:** 754–757.
47. Best Rocha A, Stroberg E, Barton LM, *et al*. Detection of SARS-CoV-2 in formalin-fixed paraffin-embedded tissue sections using commercially available reagents. *Lab Invest* 2020; **100:** 1485–1489.
48. Basso C, Aguilera B, Banner J, *et al*. Guidelines for autopsy investigation of sudden cardiac death: 2017 update from the Association for European Cardiovascular Pathology. *Virchows Arch* 2017; **471:** 691–705.

SUPPLEMENTARY MATERIAL ONLINE

A. Gross findings

B. Criteria and scoring of pathological parameters

C. SARS-CoV-2 RT-PCR methodology and results

D. *In-situ* Hybridization (ISH) methodology

E. Electron microscopy (EM) methodology

F. Results of *post hoc* tests